

Retained ratio of reinforcement in SAC305 composite solder joints: Effect of reinforcement type, processing and reflow cycle

Guang Chen ^{1,2}, Li Liu², Vadim V. Silberschmidt ², Y.C. Chan ³, Changqing Liu^{2*},
Fengshun Wu ^{1*}

1. — State Key Laboratory of Materials Processing and Die & Mould Technology, Huazhong University of Science and Technology, Wuhan 430074, China.
2. — Wolfson School of Mechanical and Manufacturing Engineering, Loughborough University, LE11 3TU, UK.
3. — Department of Electronic Engineering, City University of Hong Kong, Tat Chee Avenue, Kowloon Tong, Hong Kong.

Contact details

Guang Chen : G.CHEN2@lboro.ac.uk

LiLiu: L.Liu2@lboro.ac.uk

Vadim V. Silberschmidt:V.Silberschmidt@lboro.ac.uk

Y.C. Chan:EEYCCHAN@cityu.edu.hk

C.Q. Liu: C.Liu@lboro.ac.uk

Fengshun Wu: fengshunwu@hust.edu.cn

1 **Abstract**

2 **Purpose** – The effect of reinforcement type, processing methods and reflow cycle on
3 actual retained ratio of foreign reinforcement added in solder joints was
4 systematically studied.

5 **Design/methodology/approach** – Two kinds of composite solders based on SAC305
6 (wt.%) alloys with reinforcements of 1 wt.% Ni and 1 wt.% TiC nano-particles were
7 produced using powder metallurgy and mechanical blending method. The
8 morphology of prepared composite solder powder and solder pastes were examined;
9 retained ratios of reinforcement (RRoR) added in solder joints after different reflow
10 cycles were analysed quantitatively using an Inductively Coupled Plasma optical
11 system (ICP-OES Varian-720). The existence forms of reinforcement added in solder
12 alloys during different processing stages were studied using SEM, XRD and EDS.

13 **Findings** –The obtained experimental results indicated that the RROR in composite
14 solder joints decreased with the increase in the number of reflow cycles but a loss
15 ratio diminished gradually. It was also found that the RRORwhich could react with
16 the solder alloy were higher than that of the one that are unable to react with the
17 solder. In addition, compared with mechanical blending, the RRORs in the composite
18 solders prepared using power metallurgy were relatively pronounced.

19 **Originality/Value** –Present study offer a preliminary understanding on actual content
20 and existence form of reinforcement added in a reflowed solder joint, which would
21 also provide practical implications for choosing reinforcement and adjusting
22 processing parameters in the manufacture of composite solders.

23 **Key words:** Electronic materials; Composite materials; Solder; Retained ratio;
24 Reflow cycles

25 **1. Introduction**

26 Lead-containing solders have been continuously replaced in electronics packing
27 because of the environmental and health concerns; thus, lead-free solders
28 demonstrated a rapid development ([Abteu and Selvaduray, 2000](#); [Zhang *et al.*, 2012](#);
29 [Shen and Chan, 2009](#)). To further enhance the performance of lead-free solder joints
30 in harsh service conditions, incorporation of reinforcements into a solder matrix is
31 widely regarded as a feasible method ([Chellvarajoo, 2015](#); [Fouda and Eid, 2015](#);
32 [El-Daly *et al.*, 2013](#); [Hu *et al.*, 2013](#); [Bukat *et al.*, 2013](#); [Gao *et al.*, 2010](#)).

33 At present, there are two common methods to prepare composite solders with
34 added reinforcements: mechanical blending and powder metallurgy ([Shen and Chan,
35 2009](#); [Liu *et al.*, 2013](#); [Tsao *et al.*, 2012](#)). In the former, a solder paste and
36 reinforcement are directly mixed together through mechanical stirring. In the latter, a
37 solder powder and reinforcement are blended by ball milling before compacting,
38 sintering and subsequent extrusion or rolling. However, no matter what method is
39 used, most of the reinforcement added was excluded outside of solder joints in the
40 soldering process ([Liu *et al.*, 2008](#); [Chen *et al.*, 2015](#)). In such a case, the amount of
41 reinforcement retained in the final state of solder joints is quite different from the
42 initial one, leading to reduction of an enhancing effect due to limited doping with
43 reinforcement. To date, although the effect of foreign reinforcement on microstructure

44 and performance of lead-free solders was widely studied, a retained ratio of
45 reinforcement in composite solder joints was only mentioned in few works (Chen *et*
46 *al.*, 2016; Haseeb *et al.*, 2014; Tay *et al.*, 2013; Haseeb *et al.*, 2011). It is expected that
47 a type of reinforcements, a number of reflow cycles and a method of processing of
48 composite solders have important impacts on RRoR in solder joints.

49 In this paper, Ni and TiC nanoparticles were chosen as reinforcements to
50 strengthen a SAC matrix since Ni is known as an active reinforcement that could react
51 with molten SAC solder, while TiC is a relatively inert reinforcement (Chellvarajoo,
52 2015; Tay *et al.*, 2013; Kennedy *et al.*, 2001). To understand the effect of processing
53 and reflow cycles on RRoRs in solder joints, mechanical blending and powder
54 metallurgic routes were adopted to produce composite solders while the number of
55 reflow cycles was controlled when preparing solder joints. In addition, the
56 microstructures and chemical compositions of prepared composite solders at different
57 processing stages were contrastively investigated.

58 **2. Experimental procedures**

59 The SAC305 (wt.%) solder paste (Beijing Compo, China) and powders (Suzhou
60 EUNOW Electronic Materials, China) were used as matrix materials, while the
61 as-purchased nano-sized Ni (with an average diameter of 20 nm, JCNANO) and TiC
62 (with an average diameter of 25 nm, JCNANO) were employed as reinforcement
63 materials.

64 The initial weight fraction of both reinforcements was chosen as 1 wt. %. In this

65 paper, mechanical blending method (Method A) and a powder-metallurgy method
66 (Method B) were utilised to prepare composite solders. Specifically, in Method A, the
67 pre-weighed solder paste and the reinforcements were first mechanically blended
68 prior to printing onto an aluminium oxide chip using a steel stencil and further
69 soldering into solder balls in a reflow oven (see Fig 1a). In Method B, a mixture of a
70 solder powder and reinforcements was first ball-milled for 20 hours before uniaxial
71 compacting into solder billets and sintering at 180°C for 3 hours under vacuum
72 atmosphere. Subsequently, the sintered solder billets were rolled into solder foils (200
73 µm in thickness) and then cut into solder flakes with dimension of 1 mm×1 mm×0.2
74 mm using a rotary cutter; solder balls with an average diameter of 750 µm were
75 prepared through the reflow process (see Fig. 1a). To ensure the stability of reflow
76 process, same reflow parameters were adopted for both of method A and method B;
77 the reflow curve is shown in Fig 1b. According to the type of reinforcement added and
78 the processing method, these prepared composite solder balls are denoted as follows:
79 SAC/Ni-A, SAC/Ni-B, SAC/TiC-A and SAC/TiC-B.

80 To study the characteristics of treated composite solder (including solder paste
81 and powder) before reflow process, the morphology of and the distribution of
82 reinforcements in composite solders were observed using an environmental scanning
83 electron microscope (ESEM Quanta 200). To measure the extent of RRoRs in
84 composite solder foils and pastes before sintering and reflow, 50 mg mixture for each
85 solder were ultrasonically dissolved in aqua regia; the resultant solutions were tested
86 using an ICP-OES Varian-720 with test precision at a ppm level. The RRoRsin

87 reflowed solder joints were similarly tested using ICP-OES; 20 solder joints for each
88 group were tested to ensure the reliability of testing data. The RRoRs were quantified
89 based on an atomic weight fraction of Ni and Ti in the aqua regia solutions. For
90 microstructural analysis, the samples at different treatment stages (including before
91 sintering, after it and after reflowing) were mechanically grinded and polished for
92 observation with ESEM. In addition, the chemical composition of solder balls and the
93 phase composition of different composite solders was analysed with ICP-OES, energy
94 Dispersive Spectrometer (EDS) and X-ray diffractometer (XRD) of Phillips
95 XRD-X'Pert PRO.

96 **3. Results and discussion**

97 [Fig 2](#) shows the morphology of both plain and composite solder powder before
98 and after ball-milling process (namely, method B). It can be seen that SAC solder
99 particles show a regular spherical shape before ball-milling, while the obvious
100 collision deformation was observed on the surface of ball-milled solder particles.
101 Similarly, this change in shape of solder particles was also found in composite solder
102 particles containing Ni and TiC reinforcements. However, there are still some
103 differences observed on the surface of different single solder particles (shown in [Fig](#)
104 [2c, e and h](#)). It can be observed that the ball-milled plain SAC solder particles present
105 a relatively smooth surface. By contrast, the composite solder particles containing
106 foreign reinforcements show a relatively rough surface with a large number of dents
107 and small particles. EDS results shown in [Fig 2f and i](#) further confirmed these

108 particles adhered or embedded on surface of solder particles are the added
109 reinforcements (namely, Ni and TiC).

110 The SEM images of plain and composite solder pastes prepared by Method Aare
111 shown in Fig 3; spherical solder particles and flux can be found in plain SAC solder
112 paste. In comparison to plain SAC solder paste, the reinforcements added can be
113 observed in composite solder pastes containing Ni and TiC reinforcements, which
114 were shown in Fig 3c, d e and f. Specifically, these reinforcements added not only
115 adhere to the surface of solder particles but also exist in solder flux. To verify the
116 existence and content of foreign reinforcements in solder pastes, six different areas
117 selected were tested by EDS, relevant testing results are presented in Table 1. The
118 EDS results confirmed the existence of reinforcements in composite solder pastes; it
119 also reveals that most reinforcements added are more likely located at solder flux
120 rather than surface of solder particles.

121 According to observation results of composite solder particles and pastes, it can
122 be found that most of reinforcements added appear in the form of aggregations in
123 composites matrices (no matter what processing methods used). Specifically, the size
124 of reinforcements' aggregations adhered on surface of solder particles ranges from
125 100 to 800 nm (see Fig 2), while their size is approximately in the range of 0.1 to 1 μm
126 in composite solder pastes (see Fig 3). This phenomenon indicates that it is difficult to
127 homogeneously disperse nano-sized reinforcements into solder particles or solder
128 pastes using mainstream processing methods. A uniformly distribution of foreign
129 reinforcements in composite materials matrix in their initial size has always been a

130 difficult topic. At present, although the effect of reinforcements on microstructures
131 and solderability of solder alloys is widely studied, the actual distribution and existing
132 forms of reinforcements added in solder matrix still need further study. As for
133 processing methods, it is necessary to point out that the retained ratio of foreign
134 reinforcement in composite solders prepared by Method B might relatively lower than
135 that of composites prepared by Method A.

136 This point of view was verified after testing the actual retained ratios of Ni and
137 TiC in composite solder foils and pastes using ICP-OES; the ICP results are shown in
138 [Table 2](#). From the ICP testing data, it can be concluded that no matter what kinds of
139 reinforcements added, actual retained ratios of reinforcements in composites prepared
140 by Method A are higher than that made by Method B. For method B, the loss of
141 reinforcement might be caused by two reasons. On the one hand, the reinforcements
142 added would stick to the surface of ball-milling media (including milling jars and
143 milling balls). On the other hand, in addition to the embed or adhered reinforcements
144 on the surface of solder particles, a considerable part of reinforcements are more
145 likely to drop from the surface of solder particles during ball-milling process since
146 there was no enough strong bonding strength between solder particles and the added
147 reinforcement (especially, the inert reinforcement). The drop of reinforcements from
148 surface of solder particles also generates a large number of dents on the surface of
149 solder particles. For Method A, as shown in [Fig 3](#), the reinforcements added would
150 uniformly blend with solder flux after stirring for a long enough time (>30min),
151 leading to a higher retained ratio of reinforcement in composite solder paste.

152 The obtained testing results mentioned above clearly show that actual RROR in
153 solder pastes are higher than solder foils. However, from a practical point of view,
154 actual retained ratio and distribution form of reinforcement in a reflowed solder joint
155 are more implicational to understand the effect of doping of foreign reinforcements on
156 performance of solder joints. [Table 3](#) lists the retained ratio of reinforcements added
157 in solder joints prepared by different processing methods after different reflow cycles.
158 The ICP-OES results demonstrate a decrease of the RRoRs with the number of reflow
159 cycles for all the studied groups. Further, the retained ratios of all the groups
160 decreased significantly after the first reflow cycle. Specifically, the levels of RRoRs in
161 the solder joints for SAC/Ni-A, SAC/Ni-B, SAC/TiC-A, and SAC/TiC-B decreased
162 from the initial magnitude of 0.823%, 0.762%, 0.809% and 0.736% to 0.245%,
163 0.365%, 0.145%, and 0.176%, respectively. In particular, the retained ratio of TiC
164 reinforcement in the SAC-TiC-A group showed the most considerable reduction after
165 reflow process (the loss ratio of TiC reached up to 82.1%). However, the RRoRs saw
166 only a slight decrease when solder joints were subjected to more reflow cycles.

167 In addition to these trends, two other findings from the ICP-OES results are
168 worth mentioning. On the one hand, for the same kind of reinforcement, its loss ratio
169 in the composite solder prepared with Method B was lower than that for Method A
170 after soldering. This phenomenon could be associated with the solder paste which
171 contained flux, most of the reinforcement added was excluded from the paste as the
172 flux volatilized in the early stage of soldering, causing a substantial decline in the
173 RRoR in the final state of solder joints. However, this process of flux volatilization

174 was avoided in preparation of composite solders with Method B. Thus, the RRoR in
175 the composite solder prepared with powder metallurgy was higher after the first
176 reflow cycle.

177 On the other hand, after comparing the ICP results of two different types of
178 reinforcements, for any method employed to prepare the composite solder, the
179 retained ratio of active reinforcement (e.g. Ni) in the final solder balls were
180 obviously higher than that of inert reinforcements (e.g. TiC). Specifically, the level of
181 RRoR of Ni was always higher than that of TiC in solder balls under the same
182 conditions. A possible reason for this phenomenon is that Ni reacts readily with
183 molten Sn-Ag-Cu alloy, forming Ni-containing intermetallic compounds (IMCs). By
184 contrast, as a ceramic material, TiC is difficult to wet reactively by the molten
185 Sn-based solder during the reflowing process; a relatively higher interfacial tension
186 between TiC reinforcement and the molten solder caused the TiC reinforcements to be
187 expelled from the solder joints. It is also believed that a part of Ni reinforcement
188 reacted with SAC solder powder (resulting in Sn-Ni IMCs) at the compacting and
189 sintering stages. This part of Ni reinforcement was thus retained in solder joints in the
190 form of these IMCs. In addition, another part of Ni reinforcement that did not react
191 during sintering is expected to react with molten solder during the reflow process and
192 form new Sn-Ni and Sn-Ni-Cu IMCs. The XRD patterns of a SAC/Ni-B solder billet
193 at different treating stages (Fig. 4a) also validated this finding. However, as seen in
194 Fig. 4b, there were no new Ti-containing IMCs formed in SAC/TiC-B samples at the
195 same treating stages.

196 In addition, to further understand the existing form of reinforcements in
197 composite solders prepared by method B, the microstructures of SAC/Ni-B and
198 SAC/TiC-B composite solders were examined using SEM. The obtained SEM images
199 for two composite solders before and after sintering are shown in Fig 5 and Fig 6,
200 respectively. It can be seen in Fig 5b that there are some small grey particles with
201 spherical shape formed on the surface of Ni aggregation. These newly formed
202 particles are regarded as Sn-Ni IMCs, which were generated from inter-diffusion
203 between Sn and Ni atoms during compacting process. By contrast, in addition to the
204 initial added TiC reinforcement, no new phases were formed in SAC/TiC-B solder
205 matrix before sintering. This statement can also be confirmed by XRD results shown
206 in Fig 4.

207 Additionally, to further study the transformation of reinforcements added in
208 composite solders' matrices, microstructures of composite solders after sintering were
209 also investigated using SEM and EDS (see Fig 6). According to Fig 6, the distribution
210 forms of foreign reinforcements in solder matrices could be mainly grouped into three
211 types: a. located at crevice between three solder particles (shown in Fig 6a and d); b.
212 located at the boundary between two solder particles (shown in Fig 6b and e); c.
213 inevitably aggregated at the defect location resulted from the irregular shape of solder
214 particles after ball-milling. From the obtained SEM images, the initial distribution
215 forms of added reinforcements (especially, the active reinforcement - Ni) would
216 largely affect their existing form in solder matrices after sintering. For the first two
217 distribution forms, Ni reinforcements are more likely to entirely transform into Sn-Ni

218 or Sn-Ni-Cu IMCs after sintering, which can be seen in Fig 6a and b. However, for
219 the third distribution form, the Ni reinforcements added would not entirely transform
220 into Ni contained IMCs due to the relatively large size of Ni aggregation. In this case,
221 Ni contained IMCs would be formed from outside to inside around the Ni aggregation
222 (see Fig 6c). EDS results of selected points in Fig 6 are listed in Table 4. According to
223 Fig 6a, b and EDS results of point 1, 2 and 3 shown in Table 4, it can be known that
224 the IMCs formed at solder particles' boundaries are mainly Ni₃Sn₄ or Ni₃Sn₂, which
225 resulted from a fully reaction between Ni reinforcements and Sn-based solder during
226 sintering. However, for the Ni aggregation with larger size, the centre of the
227 aggregation is the non-reacted Ni reinforcements, which are surrounded by newly
228 formed Ni-contained IMCs. The content of Ni element in inner side of the IMCs
229 layer is proved higher than in outer side (see EDS results of point 4, 5, 6 and 7). In
230 contrast, the TiC reinforcement remains its initial morphology and distribution forms
231 in SAC/TiC composite solder matrix without new IMCs formed, which could also be
232 evidenced by relevant XRD, SEM and EDX results. By comparing the SEM images
233 of the two studied solder alloys after reflowing (shown in Fig 7), it can also be found
234 that blocky Ni-Sn-Cu IMCs were formed in the matrix of the SAC/Ni composite
235 solder alloy, indicating that Ni remained in the solder joints in the form of
236 Ni-containing IMCs. Still, no similar phenomenon was found in the reflowed
237 SAC/TiC solder alloy, and the TiC reinforcement exists in the solder matrix in its
238 initial state without any new phase formed

239 The big difference in transformation of Ni and TiC reinforcements in solder

240 matrices during compacting, sintering and reflowing process could be explained by
241 different physical attributes of two reinforcements. As mentioned above, Ni is an
242 active metal reinforcement, which is much easier to react with solid or molten
243 Sn-based solder alloy by atom diffusion under mechanical loading or heating
244 condition. On the contrary, as a typical ceramic material, TiC reinforcement can
245 hardly build a reliable bonding with solid or molten solder alloy due to the non-wetted
246 interface and relatively higher interfacial tension during processing process
247 (especially, sintering and reflowing). Essentially, the relatively stable interface
248 between TiC and solder matrix is mainly determined by the difference in chemical
249 bond structure between ceramic materials and metal materials. Actually, in addition to
250 the proposed factors in the present study (including type of reinforcement, processing
251 methods and reflow cycles), other factors such as density of reinforcements,
252 modification of reinforcement, alloy elements and soldering approaches might also
253 have important effects on retained ratio of foreign reinforcements in solder
254 interconnections; these aspects would be also valuable and instructive in follow-up
255 study.

256 **4. Conclusions**

257 The retained ratios of two kinds of reinforcement in the SAC based composite
258 solder joints decrease with the reflow cycles. The loss the reinforcements reached
259 their maximum after the first reflow for both reinforcements. In addition, the loss
260 ratios showed a much slower decline for the subsequent reflow cycles. For the same

261 reinforcement, the levels of its retained ratio in the composite solder prepared with
262 powder metallurgy were higher than those prepared with the solder-paste blending
263 method. For the same processing method, the retained ratio of active reinforcement –
264 Ni – that could react with the solid and molten solder was higher than that of TiC
265 reinforcement which is unable to react with solder alloy.

266 **Acknowledgments**

267 The authors acknowledge the research funding by the National Nature Science
268 Foundation of China (NSFC) (NSFC NO. 61261160498). This research was also
269 supported by China-European Union technology cooperation project, No. 1110 as
270 well as Marie Curie International Research Staff Exchange Scheme Project within the
271 7th European Community Framework Programme, No. PIRSES-GA-2010-269113,
272 entitled “Micro-Multi-Material Manufacture to Enable Multifunctional Miniaturised
273 Devices (M6)”.

274 **Reference**

- 275 Abtew, M and Selvaduray, G. (2000), “Lead-free solders in microelectronics”, *Mater*
276 *Sci Eng R*, Vol. 27, pp. 95-141.
- 277 Zhang, L., He, C.W., Guo, Y.H., Han, J.G., Zhang, Y.W. and Wang, X.Y. (2012),
278 “Development of SnAg-based lead free solders in electronics packaging”,
279 *Microelectron Reliab*, Vol. 52, pp. 559-578.
- 280 Shen, J. and Chan, Y.C. (2009), “Research advances in nano-composite solders”,

281 *Microelectron Reliab*, Vol. 49, pp. 223-234.

282 Chellvarajoo, S., Abdullah, M.Z. and Khor, C.Y. (2015), “Effects of diamond
283 nanoparticles reinforcement into lead-free Sn–3.0Ag–0.5Cu solder pastes on
284 microstructure and mechanical properties after reflow soldering process”, *Mater*
285 *Design*, Vol. 82, pp. 206-215.

286 Fouda, A.N. and Eid, E.A. (2015), “Influence of ZnO nano-particles addition on
287 thermal analysis, microstructure evolution and tensile behavior of Sn–5.0wt%Sb–
288 0.5wt% Cu lead-free solder alloy”, *Mater Sci Eng A*, Vol. 632, pp. 82-87.

289 El-Daly, A.A., Hammad, A.E., Fawzy, A. and Nasrallah, D. A. (2013), “Microstructure,
290 mechanical properties, and deformation behavior of Sn–1.0Ag–0.5Cu solder after
291 Ni and Sb additions”, *Mater Design*, Vol. 43, pp. 40-49.

292 Hu, X., Chan, Y.C., Zhang, K.L. and Yung, K.C. (2013), “Effect of graphene doping
293 on microstructural and mechanical properties of Sn–8Zn–3Bi solder joints
294 together with electromigration analysis”, *J Alloy Compd*, Vol.580, pp.162-171.

295 Bukat, K., Sitek, Janusz., Koscielski, M., Niedzwiedz, W., Mlozniak, A. and
296 Jakubowska, M. (2013), “SAC solder paste with carbon nanotubes. Part II: carbon
297 nanotubes’ effect on solder joints’ mechanical properties and microstructure”,
298 *Solder Surf Mt Tech*, Vol. 25, pp. 195-208.

299 Liu, X.D., Han, Y.D., Jing, H.Y., Wei, J. and Xu, L.Y. (2013), “Effect of graphene
300 nanosheets reinforcement on the performance of Sn–Ag–Cu lead-free solder”,
301 *Mater Sci Eng A*, Vol.562, pp.25-32.

302 Gao, L.L., Xue, S.B., Zhang, L., Sheng, Z., Ji, F., Dai, W., Yu, S.L. and Zeng, G.

303 (2010), “Effect of alloying elements on properties and microstructures of SnAgCu
304 solders”, *Microelectron Eng*, Vol. 87, pp. 2025-2034.

305 Tsao, L.C., Huang, C.H., Chung, C.H. and Chen, R.S. (2012), “Influence of TiO₂
306 nanoparticles addition on the microstructural and mechanical properties of
307 Sn0.7Cu nano-composite solder” *Mater Sci Eng A*, Vol.545, pp.194-200.

308 Liu, J., Andersson, C., Gao, Y. and Zhai, Q. (2008), “Recent development of
309 nano-solder paste for electronic interconnect applications”, Proceedings of the
310 10th Electronics Packaging Technology Conference, Singapore, pp. 84–93.

311 Chen, G., Wu, F.S., Liu, C.Q. and Chan, Y.C. (2015), “Effect of fullerene-C60&C70
312 on the microstructure and properties of 96.5Sn-3Ag-0.5Cu solder”, 65th
313 Electronic Components & Technology Conference, U.S., pp.1262-1267.

314 Chen, G., Huang, B.M., Liu, H., Chan, Y.C., Tang, Z.R. and Wu, F.S. (2016), “An
315 investigation of microstructure and properties of Sn3.0Ag0.5Cu-XAl₂O₃
316 composite solder”, *Solder Surf Mt Tech*, Vol. 28, pp. 84-92.

317 Haseeb, A.S.M.A., Leong, Y.M. and Arafat, M.M. (2014), “In-situ alloying of
318 Sne3.5Ag solder during reflow through Zn nanoparticle addition and its effects on
319 interfacial intermetallic layers”, *Intermetallics*, Vol. 54, pp. 86-94.

320 Tay, S.L., Haseeb, A.S.M.A., Johan, M.R., Munroe, P.R. and Quadir, M.Z. (2013),
321 “Influence of Ni nanoparticle on the morphology and growth of interfacial
322 intermetallic compounds between Sne3.8Ag0.7Cu lead-free solder and copper
323 substrate”, *Intermetallics*, Vol. 33, pp. 8-15.

324 Haseeb, A.S.M.A. and Leng, T. S. (2011), “Effects of Co nanoparticle addition to

325 Sn-3.8Ag-0.7Cu solder on interfacial structure after reflow and ageing”,

326 *Intermetallics*, Vol. 12, pp. 707-712.

327 Kennedy, A.R. and Wyatt, S.M. (2001), “Characterizing particle–matrix interfacial

328 bonding in particulate Al–TiC MMCs produced by different methods”, *Compo Pt*

329 *A*, Vol. 32, pp. 555-559.

330

331

332

333

334

335

336

337

338

339

340 **List of Figures**

341 **Fig. 1** (a) Schematic diagram of processing methods (b) Reflow condition for

342 preparing solder balls

343 **Fig 2** morphology of both plain and composite solder powder after ball-milling

344 process: (a-c) for SAC, (d-f) for SAC/Ni and (g-i) for SAC/TiC.

345 **Fig 3** Morphology of both plain and composite solder pastes: (a-b) for plain SAC,

346 (c-d) for SAC/Ni and (e-f) for SAC/TiC.

347 **Fig. 4** XRD patterns of SAC/Ni (a) and SAC/TiC (b) composite solders at different
348 treating stages

349 **Fig 5** Microstructures of (a-b) SAC/Ni and (c-d) SAC/TiC composite solders prepared
350 through method B before sintering

351 **Fig 6** Microstructures of (a-c) SAC/Ni and (d-f) SAC/TiC composite solders prepared
352 through method B after sintering.

353 **Fig. 7** Microstructures of (a) SAC/Ni and (b) SAC/TiC composite solders after reflow.

354

355

356

357

358

359

360

361

362 **List of tables**

363 **Table 1** Weight percentage of different Elements of selected areas in Fig 3

364 **Table 2** Actual weight fraction of reinforcements in composite solder foils and pastes
365 before reflow

366 **Table 3** Reinforcement elements in different solder balls tested by ICP-OES

367 **Table 4** Atoms percentage of different elements of selected points in Fig 8

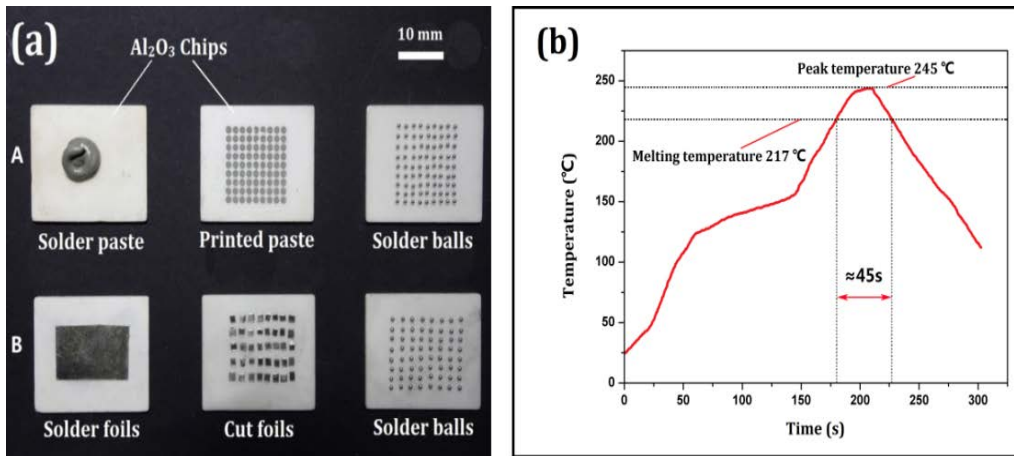


Fig. 1 (a) Schematic diagram of processing methods (b) Reflow condition for preparing solder balls

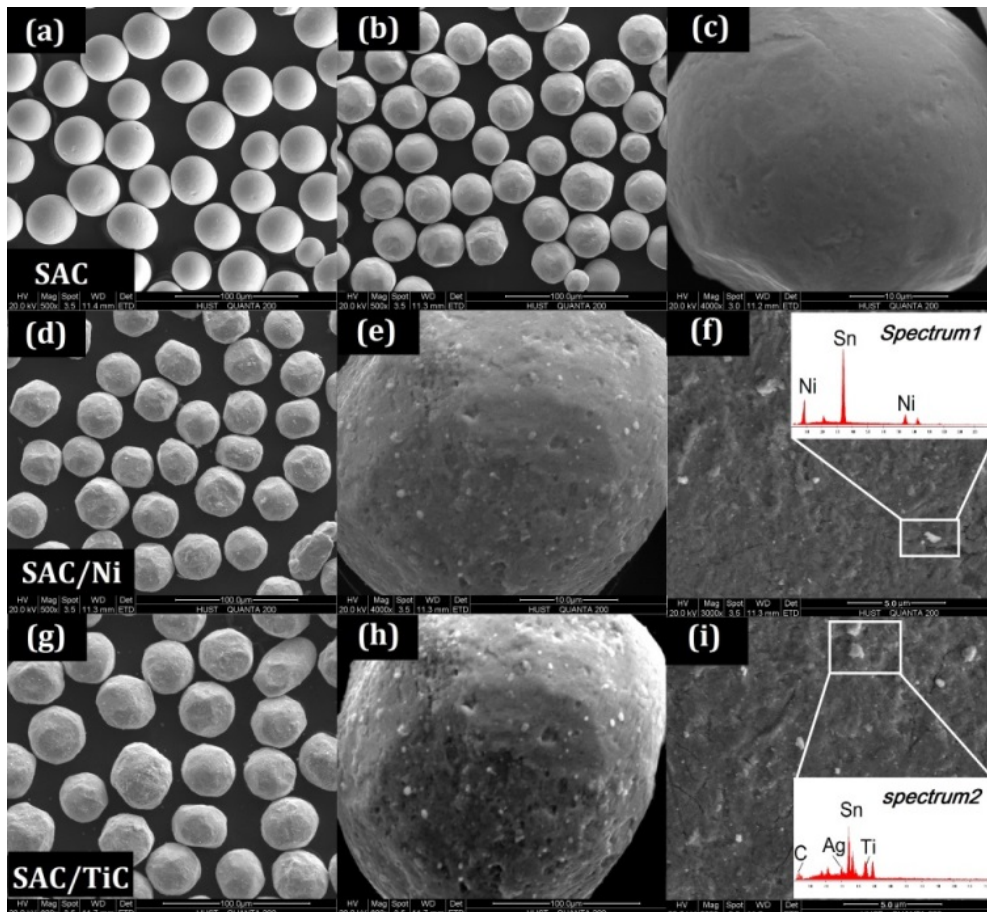


Fig 2 morphology of both plain and composite solder powder after ball-milling process: (a-c) for SAC, (d-f) for SAC/Ni and (g-i) for SAC/TiC.

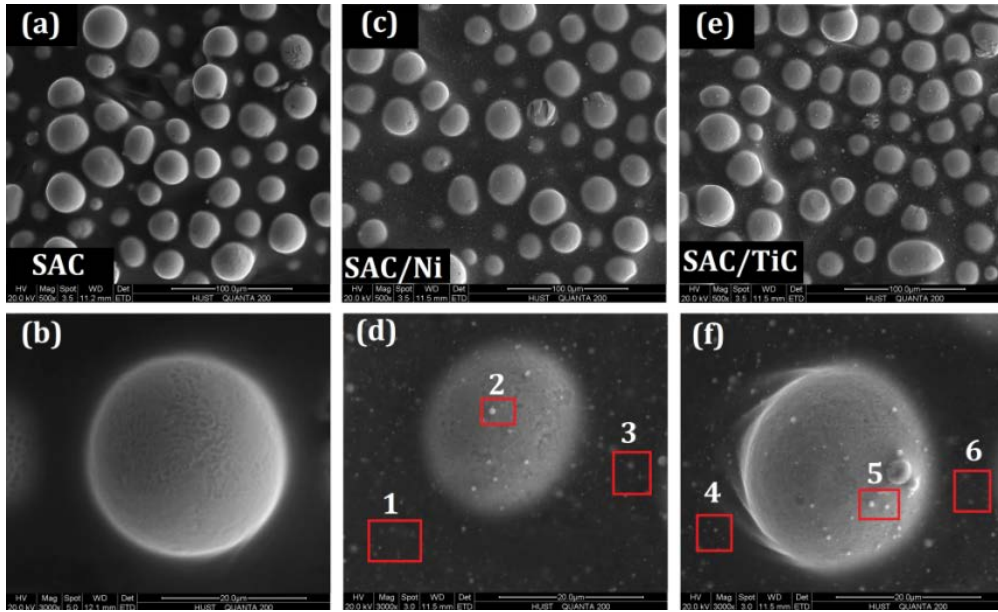


Fig 3 Morphology of both plain and composite solder pastes: (a-b) for plain SAC, (c-d) for SAC/Ni and (e-f) for SAC/TiC.

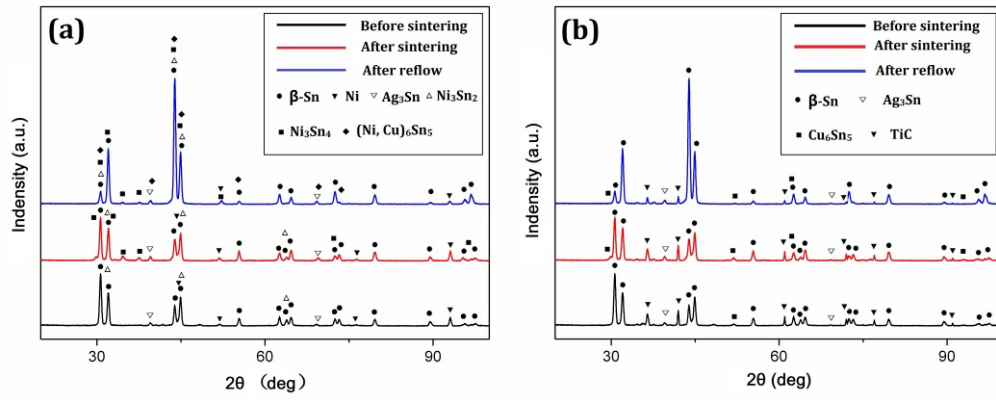


Fig. 4 XRD patterns of SAC/Ni (a) and SAC/TiC (b) composite solders at different treating stages

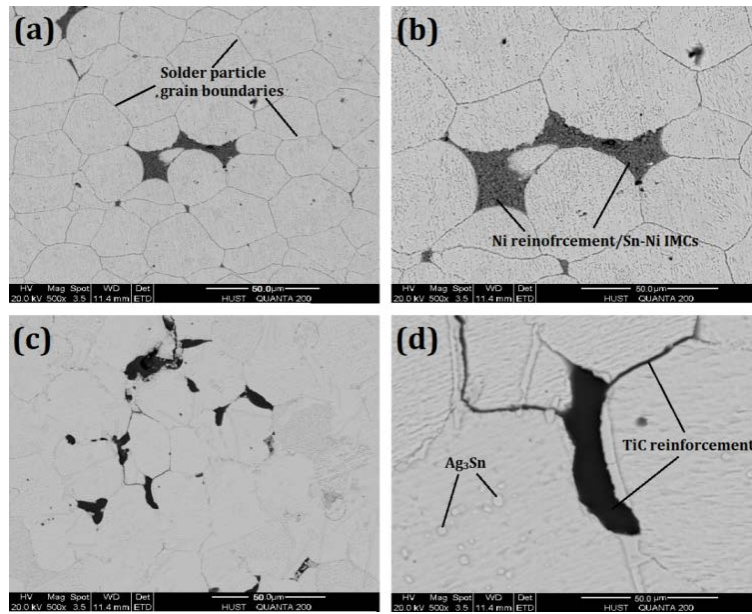


Fig 5 Microstructures of (a-b) SAC/Ni and (c-d) SAC/TiC composite solders prepared through method B before sintering

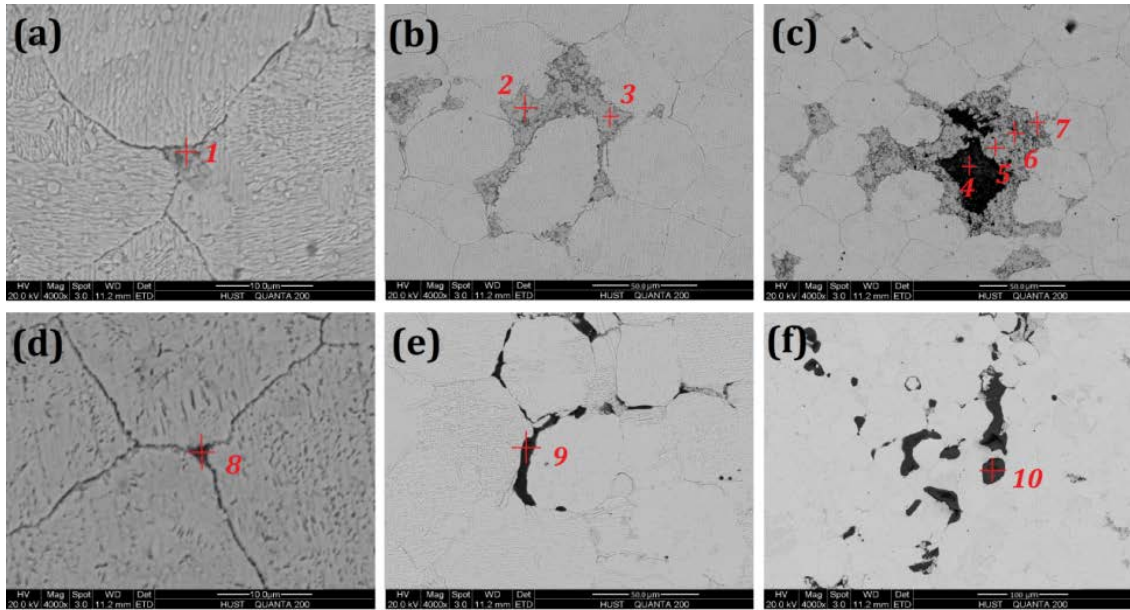


Fig 6 Microstructures of (a-c) SAC/Ni and (d-f) SAC/TiC composite solders prepared through method B after sintering.

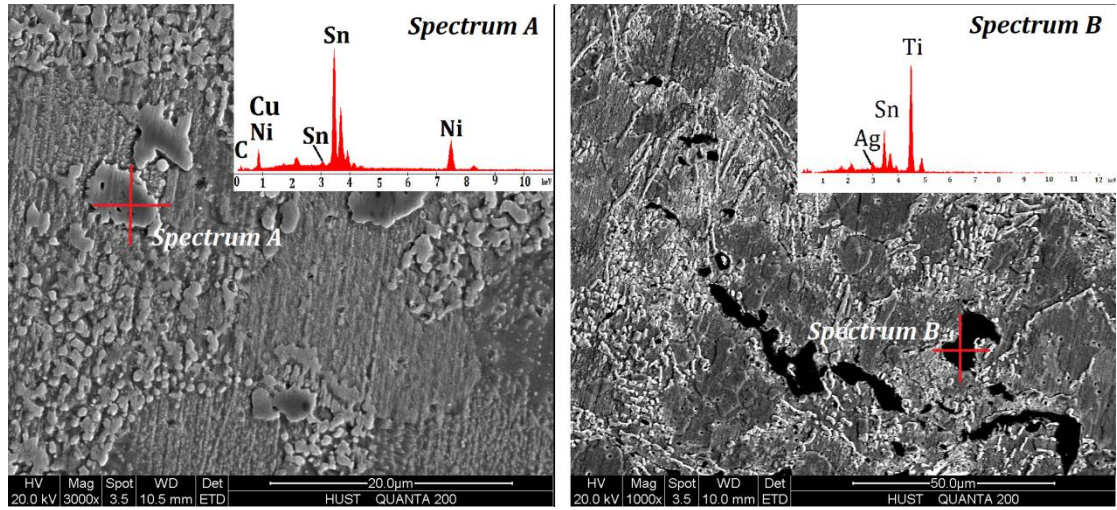


Fig. 7 Microstructures of (a) SAC/Ni and (b) SAC/TiC composite solders after reflow.

Table 1 Weight percentage of different Elements of selected areas in Fig 3

	Sn (wt. %)	Ag (wt. %)	Cu (wt. %)	Ni (wt. %)	C (wt. %)	Ti (wt. %)
#1	9.82	—	—	7.38	82.8	—
#2	79.3	1.8	0.27	1.2	17.43	—
#3	8.89	—	—	6.92	84.19	—
#4	7.78	0.07	—	—	87.8	4.35
#5	83.6	2.1	0.06	—	13.19	1.05
#6	8.92	—	—	—	88.7	2.38

Table 2 Actual weight fraction of reinforcements in composite solder foils and pastes before reflow

Solder type	Wt .% of Ni		Wt .% of TiC	
	SAC/Ni-A	SAC/Ni-B	SAC/TiC-A	SAC/TiC-B
Reference	1	1	1	1
RROR	0.823	0.762	0.809	0.736

Table 3 Reinforcement elements in different solder balls tested by ICP-OES

Solder types	Reflow cycles		
	1	2	3
SAC/Ni-A	0.245%	0.186%	0.162%
SAC/Ni-B	0.365%	0.276%	0.262%
SAC/TiC-A	0.145%	0.118%	0.102%
SAC/TiC-B	0.176%	0.14%	0.128%

Table 4 Atoms percentage of different elements of selected points in Fig 8

	Sn (At. %)	Ag (At. %)	Cu (At. %)	Ni (At. %)	C (At. %)	Ti (At. %)
#1	55.47	1.08	0.24	43.21	—	—
#2	56.12	1.24	0.83	41.81	—	—
#3	57.11	1.48	0.63	40.78	—	—
#4	35.46	0.72		63.82	—	—
#5	41.21	0.28	0.19	58.32	—	—
#6	44.89	1.84	1.10	52.13	—	—
#7	68.34	1.67	0.54	29.45	—	—
#8	50.31	0.21	0.08	—	22.67	26.73
#9	48.24	0.93	0.53	—	24.58	25.12
#10	48.76	0.82	0.41	—	23.52	26.47